Research Article Open Access

Shaan Bibi Jaffri, Khuram Shahzad Ahmad*

Prunus cerasifera Ehrh. fabricated ZnO nano falcates and its photocatalytic and dose dependent *in vitro* bio-activity

Running Title: Photodegradation and antimicrobial potential of biogenic ZnO nano falcates

https://doi.org/10.1515/chem-2018-0022
received November 1, 2017; accepted January 10, 2018.

Abstract: Zinc oxide nano falcates of sickle shape have been synthesized from *Prunus cerasifera* pomological extract as a reducing cum stabilizing agent via novel, biomimetic and non-toxic route. Zinc oxide nano falcates were analyzed via ultraviolet spectroscopy, Fourier transform infrared analysis, X-ray powder diffraction, scanning electron microscopy and atomic force microscopy. Highly stable zinc oxide nano falcates synthesized at 200°C and 400°C calcination temperatures expressed intense UV-vis peak at 398 nm. Phenolic and amino groups were revealed by FTIR in pomological extract. Wurtzite crystalline structure of zinc oxide nano falcates was confirmed by XRD with average crystal size of 4.93 nm. SEM sizes ranged between 72.11-120 nm and 56.57-107.70 nm, respectively and shown higher polydispersity levels for two calcination temperatures. Augmented photocatalytic degradation of methyl red and bromophenol blue under direct solar irradiance shown pseudo first order kinetics (R^2= 0.99 and 0.96). Furthermore, biomedical and agriculturally important pathogenic strains i.e., *Xanthomonas axonopodis* pv. *citri* and *Pseudomonas syringae*, *Aspergillus niger, Aspergillus flavus, Aspergillus fumigatus, Aspergillus terreus, Penicillium chrysogenum, Fusarium solani* and *Lasiodiplodia theobromae* were remarkably inhibited. Enhanced photocatalytic and antimicrobial activity reveals zinc oxide nano falcates promising prospects in nano bioremediation of polluted water and conversion into green nano pesticides.

Keywords: Biomaterials; Photochemistry; Environmental chemistry; Chemical kinetics and reactivity; Catalysis; Analytical chemistry.

1 Introduction

Modern age is essentially being dominated by nanotechnology, which has emerged as a novel technology by provisioning the advanced materials of nano range of medicinal and commercial importance. ZnO is a semi-conductor (II-IV) of wide band gap, has an energy band gap of 3.37 eV. Among metallic nanoparticles (NPs), ZnO NPs have been used in myriad of catalytic applications for larger surface area [1]. ZnO as a catalyst has been synthesized on commercial scale for agrarian, skin protection and beautifying purposes owing to its antimicrobial and anti-oxidant properties [2-4]. ZnO NPs have been synthesized via physical and chemical routes posing challenges in terms of environmental toxicity and complicated operating conditions. Thus, ZnO NPs via plant biomimetic route has been employed as a green and novel method for last few decades. Phytosynthetic route for ZnO NPs is ecologically safe and cost effective demonstrating its potential for substitution of chemical and physical routes [5,6].

Prunus cerasifera Ehrh. (*P. cerasifera*) also named as cherry plum is an angiospermic plant belonging to family Rosaceae. *P. cerasifera* is an important medicinal plant. All prune fruits are reservoirs of phytochemicals i.e., polyphenols, anthocyanins, carotenoids, flavonoids, acids of organic make up, fibrous and enzymatic content, benzene containing compounds, tannins, minerals (K, P, Ca, Mg) and Vit. A, B, C and K [7]. *P. cerasifera* fruit also has considerable phenolic content, many types of anthocyanins and antioxidant components [8]. Various

***Corresponding author: Khuram Shahzad Ahmad,** Department of Environmental Sciences, Fatima Jinnah Women University, The Mall, 46000, Rawalpindi, Pakistan, E-mail: chemist.phd33@yahoo.com
Shaan Bibi Jaffri: Department of Environmental Sciences, Fatima Jinnah Women University, The Mall, 46000, Rawalpindi, Pakistan

types of anthocyanins found in *P. cerasifera* fruit are cyanidin-3-galactoside, cyanidin-3-xyloside, cyanidin-3-glucoside, cyanidin-3-rutinoside, peonidin-3-glucoside, peonidin-3-rutinoside, pelargonidin-3-glucoside and yanidin-3-(6"-acetoyl) glucoside [9]. Phenolic content like quercetin, quercetin glucoside, quercetin rutinoside, quercetin arabinopyranosyl, epicatechin, procyanidin C, chlorogenic acid, xyloside, catechin, procyanidin B_1, quercetin galactoside and procyanidin B_2 has been found in *P. cerasifera* fruit [10].

ZnO nanoparticles have been synthesized with reducing phytochemicals of different plants. However, studies regarding ZnO nanoparticles synthesized from *P. cerasifera* is nonexistent. Herein, ZnO nano falcates phytosynthesized from reducing agents of *P. cerasifera* fruit has been reported. Pomosynthetic (fruit mediated) ZnO nano falcates (PZO NFs) have been characterized via UV-vis, FTIR, SEM, XRD and AFM. Furthermore, PZO NFs were analyzed for their photocatalytic potential in degrading methyl red (MR) and bromophenol blue (BB) dyes direct solar irradiance exploiting its nano-bioremediation potential. Dose dependent in vitro biological activity of PZO NFs was evaluated for bacterial and fungal strains i.e., *X. citri*, *P. syringae*, *A. niger, A. flavus, A. fumigatus, A. terreus, P. chrysogenum, F. solani* and *L. theobromae*. *In vitro* biological activity of PZO NFs has been done to evaluate its favorability in terms of green nano bactericide and fungicide.

2 Experimental

2.1 Materials

Zinc nitrate, potassium bromide and nutrient agar (NA) culture media were purchased from Merck, Germany. Methyl red and bromophenol blue were purchased from BDH, England. Potato dextrose agar (PDA) culture media was purchased Liofilchem, Italy. All chemicals used in investigation were of analytical grade and have been used without further purification.

2.2 Fruit extract preparation

P. cerasifera ripened fruits were collected from trees located on farm sides in June, 2016 (summers) from Ali Zai area of Parachinar valley (latitude: 33°53'1.29"N, longitude: 70°6'35.49"E), head quarter of Kurram Agency, Federally Administered Tribal Areas, Pakistan (Figure 1a). Parachinar is famous for *P. cerasifera* production, utilized for a myriad of pharmacological and edible purposes. Fruit samples were transported to lab in tightly closed polyethylene bags. The ripened fruits exhibited yellow to reddish peel color, yellow pulp with characteristic sweet and sour taste and unique aroma similar to that of plum. For sterilization, fruit samples were washed three times with tap water for removal of deposited dust and environmental pollutants. Fruits were then spread on clean sheets in the shade for moisture removal and drying. Fruits were shade-dried for avoiding any possible phytoconstituents reaction with light. Upon complete drying, fruits were collected and washed with distilled water followed by oven drying at 100°C in Oven (UN110, Memmert, Germany). Fruits were then ground into fine powder with the help of pestle and mortar, sieved and stored in sealed polyethene bags.

For aqueous filtrate preparation, 10 g of fruit powder was weighed on weighing balance (UX6200H, Shimadzu, Japan) and extracted with 1000 mL of double distilled water in a 1000 mL conical flask. This mixture was then heated at 30°C with constant magnetic stirring on hotplate (MSH 20D, Wisestir, Germany) for 10 min. It was followed by double filtration with Whatman No. 1 filter paper (pore size: 11 µm), refrigerated at 4°C for utilization as a reducing agent in PZO NFs synthesis. The *P. cerasifera* fruit extract (PCFE) obtained was dark brown in color with characteristic cherry plum odor. The yield of doubly filtered PCFE was calculated as follows:

$$\%\, Yield = \left(\frac{W1}{W2}\right) x\ 100 \quad (1)$$

where W1 represents the PCFE weight after double filtration while W2 is the *P. cerasifera* powder taken initially. The percentage yield for 10 g of *P. cerasifera* fruit extracted with 1000 mL was estimated to be 89.88% expressing the solvent i.e., double distilled water's higher efficiency in extraction of reducing agents from *P. cerasifera*.

2.3 Pomosynthesis of ZnO nano falcates

PZO NFS were synthesized from aqueous extract of *P. cerasifera* fruit. Prior to addition of $Zn(NO_3)_2$, 30 mL of *P. cerasifera* fruit extract was boiled at 60-80°C on magnetic stirring and heating. After 20 min of heating, 3 g of $Zn(NO_3)_2$ was added in solution at 60°C. Heating and stirring of this mixture was continued till conversion of the solution to deep yellowish suspension. The paste like suspension was centrifuged at 6000 rpm (C0060-230V, Labnet International, Inc. USA) and washed with ethanol followed by placing in two ceramic crucibles for hot air

a

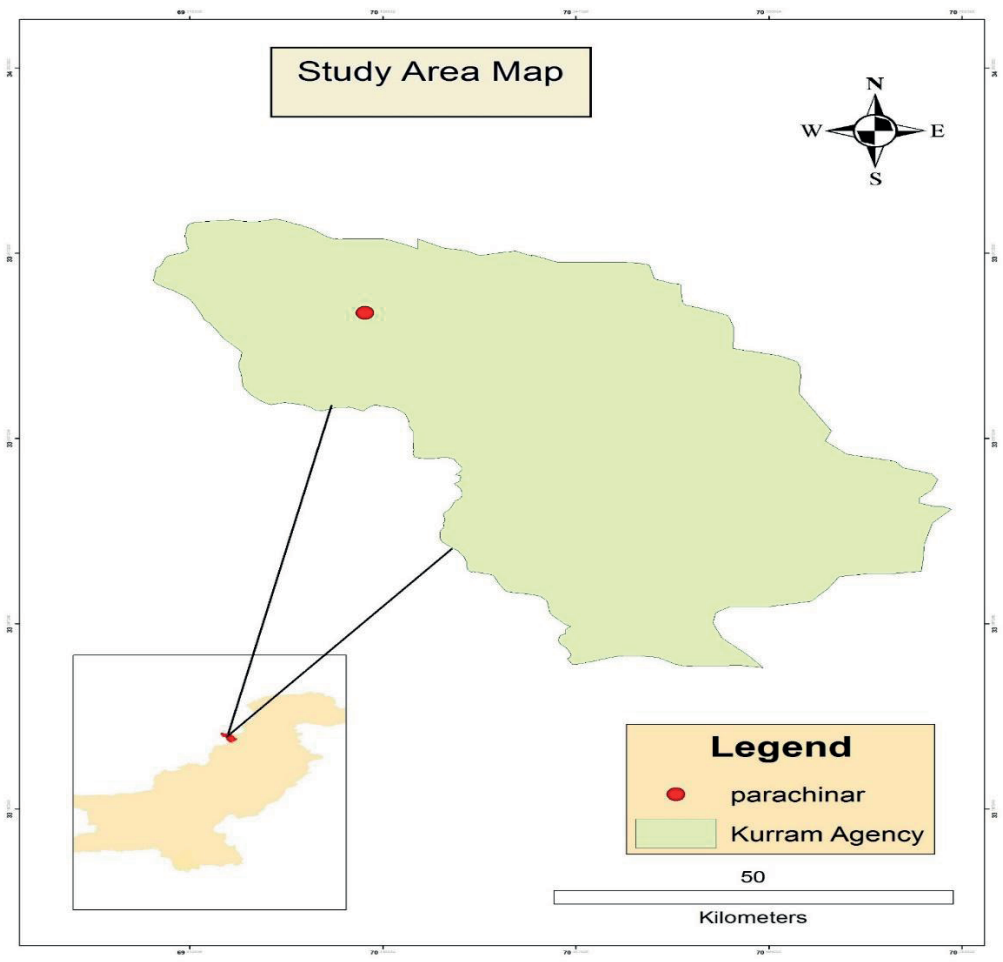

b

Figure 1: a) Map showing the administrative location of Parachinar, Kuram Agency, FATA, Pakistan and b) *P. cerasifera* fruit.

drying at 120°C in oven for 2 h [11]. Obtained products were calcinated at two temperatures i.e., 200 and 400°C for 2 h for obtaining PZO NFs furnace (D550, Ney Vulcan, USA) [12]. Calcined white powder was further ground with pestle and mortar for characterization.

2.4 Characterization

PZO NFs were analytically examined via UV-Vis spectrophotometer (1602, Biomedical services, Spain) with spectra recorded in range of 200-800 nm. The

photocatalytic dye degradation potential of PZO NFs was also monitored via UV-Vis. The interplay of functional groups was checked by Fourier Transform Infrared, FTIR spectrophotometer (8400, Shimadzu, Japan). Crystal structure of PZO NFs was characterized by Bruker AXS D-8 powder X-ray diffractometer (Shimadzu, Japan), operated at 40 kV, 20 mA, with CuKα radiation (λ = 1.5406 Å). Morphological features of PZO NFs were characterized by scanning electron microscopy (SEM JOEL JSM-6490, Germany) and atomic force microscopy (AFM (NT-MDT Solver Pro, Russia).

2.5 PZO NFs photocatalytic activity

Photocatalytic dye degradation potential of PZO NFs was examined for methyl red and bromophenol blue under direct solar irradiance for 30 min from 12:00-12:30 PM on a sunny day with an average intensity 68-73 Klux (LT300, Extech, UK). Methyl red and bromophenol blue solutions (10 mL) were separately mixed with 15 mg of PZO NFs. Degradation was monitored by UV-Vis spectrophotometer and alleviating absorbance was recorded for calculating the rate of reaction and degradation percentages by:

$$\% \text{ Degradation} = (Ai - Af / Ai) \times 100 \quad (2)$$

Where A_i represents the dyes' initial absorbance while A_f is the dyes' final absorbance after addition of PZO NFs.

2.6 Antibacterial and antifungal assay

Culturing media i.e., PDA and NA, petri plates, and filter paper discs were autoclaved and then dried in oven prior to use for all experiments. All the experiments were carried out in triplicate and the final values obtained for zone of inhibition were presented as mean values along with standard deviations. Values of $P<0.05$ were considered to indicate a statistically significant difference. Antibacterial and antifungal assays were done with the PZO NFs calcined at 400°C due to their smaller size by preparation of PZO NFs stock solution in methanol for obtaining the final concentration of 100 mg/mL and the volume used in different dose was 5, 10, 15, 20 µL. Stock solution was sonicated for 30 min and assays were strictly done within 1-2 h of sonication.

Antibacterial potential of PZO NFs was tested against *X. citri* and *P. syringae* by standard Kirby–Bauer disc diffusion assay. Prior to PZO NFs inoculation, the bacterial test strains were grown in NA broth for 24 h in incubator at 37 °C. The NA plates were prepared followed by sterilization and solidification in laminar flow cabinet (Streamline, Singapore) at 45°C. The bacterial cultures grown overnight were spread on the solidified plates with help of sterile loop for obtaining bacterial lawns. The autoclaved and dried filter paper discs were picked up with help of a sterile forcipes and inserted on NA plates. Discs on control set were loaded with 10 µL of $Zn(NO_3)_2$ salt solution, 10 µL of standard antibacterial drug Ampicillin and 10 µL *P. cerasifera* fruit extract as a control while the discs on another set of NA plates was loaded with 2, 4, 6 and 10 µL of PZO NFs with 24 h incubation time at 37°C in incubator (Sanyo MR-153, GeminiBV, Netherlands). On the next day, the zone of inhibition were measured with help of meter ruler and recorded by taking mean values in mm and compared with standard *Ampicillin*. PZO NFs were also tested for their fungicidal activity against pathogens *i.e., A. niger, A. flavus, A. fumigatus, A. terreus, P. chrysogenum, F. solani* and *L. theobromae* by standard Kirby–Bauer disc diffusion assay. The fungal organisms were grown on PDA for 72 h. Fungal culture (200 µL) was poured onto the PDA with help of sterile spreader for obtaining fungal lawns. Discs on control set were loaded with 10 µL of $Zn(NO_3)_2$ salt solution, 10 µL of standard Amphotericin B and 10 µL *P. cerasifera* fruit extract as a control while the discs on another set of PDA plates was loaded with 5, 10, 15 and 20 µL of PZO NFs and were incubated for 72 h. The zones of inhibition were noted and recorded and compared with standard Amphotericin B.

Ethical approval: The conducted research is not related to either human or animals use.

3 Results and discussion

Present research synthesized ZnO nano falcates through a complete green pathway. The synthetic route utilized the biochemicals found in *P. cerasifera* as an alternative to chemical stabilizers e.g., sodium borohydride, tri-sodium citrate, glucose. Additionally, these biochemicals capped the ZnO nano falcates thus terminating the need for chemical capping agents e.g., polyvinyl pyrrolidone, ethylenediaminetetraacetic acid, polyvinyl alcohol. However, zinc nitrate has been used as ZnO source in one pot synthesis. Since all Prunus fruits are highly rich in reducing agents thus have been utilized for biogenic synthesis of different metallic nanoparticles e.g. *P. amygdalus* [13], *P. domestica* [14], *P. persica* [15], *P. serotina* [16], *P. armeniaca* [17], *P. yedoensis* [18]. Only one research has been reported for the synthesis of ZnO with juice extract of *P. cerasus* [19], however no data has been

reported for ZnO fabrication with *P. cerasifera*. Various studies identified *P. cerasifera* growing in regions like Serbia [20], Pakistan [21], China [22] and France [23]. *P. cerasifera* in these regions has been used for biological investigations however, current investigation utilized *P. cerasifera* for facile and biomimetic synthesis of PZO NFs synthesis. *P. cerasifera* has a widespread distribution and fruits found in different regions predominantly vary in color and size. The wild as well as the cultivated *P. cerasifera* fruit distributed all over the world are highly polymorphic for various characteristics. *P. cerasifera* is exceedingly adaptable to transforming ecological conditions.

3.1 Pomoreductant role of *P. cerasifera*

Although, ZnO nanoparticles have been synthesized with variety of plant species but present investigation specifically employed *P. cerasifera* fruit for pomoreduction of PZO NFs primarily due to its highly prevalent spatial distribution, unique phytochemical composition and enhanced antimicrobial activity. *P. cerasifera* has a plenty of significant chemical resource but it is underutilized [22] making it a suitable candidate for current bioprospecting in PZO NFs one pot synthesis.

P. cerasifera (Figure 1b) occurrence in European and Asian countries in wild as well as domesticated varieties contributes to its widespread distribution. However, the sampled fruits utilized in present research represents wild variety possessing higher innate pest resistance. Thus, enhancing its availability on large scale for extraction of reducing agents for prunosynthesis of PZO NFs. *P. cerasifera* fruit is also available on commercial scale both in fresh and dried forms in all seasons.

Furthermore, *P. cerasifera* fruit was also preferred due to its exceptional chemical composition which surpasses many plant species in not only reducing but also stabilizing of PZO NFs. Dried fruit powder utilized for PZO NFs synthesis comprised of higher quantities of antioxidant phytochemicals actively involved in capping of PZO NFs. Drying augments the quantity of reducing sugars due to dehydration. *P. cerasifera* phytochemicals involved in prunosynthesis of PZO NFs are sugars (glucose, fructose, sucrose, sorbitol), amino acids (total amino acids and aspartic acid), vitamins (ascorbic acid (C), thiamin (B1), riboflavin (B2), niacin (B3), α-tocopherol (e), carotenoids (lutein, α-carotene, β-carotene), organic acids (malic and quinic acid), phenolic compounds (neochlorogenic acid, chlorogenic acid, caffeic acid, coumaric acid, anthocyanins, catechins, rutin) [24]. Total antioxidant capacity (TAC) method evaluation reveals *P. cerasifera* to possess antioxidant potential up to 0.267 mg Gallic acid equivalent (GAE) kg^{-1} [25] in addition to the polyphenol chlorogenic acid' s main contribution towards antioxidant potential.

P. cerasifera, due to its inherent antimicrobial potential against bacterial and fungal strains was utilized for augmenting the inhibition power of PZO NFs. Higher quantities of tannins in *P. cerasifera* can combine with proteins inducing the inhibition of plant microbial enzymes and viruses thus acting as natural pesticide [26,27].

3.2 Synthesis and characterization of PZO NFs

PZO NFs formation was confirmed by the yellowish colored suspension formed and later precipitation occurred during reaction. PZO NFs have shown a broad peak in range of 350-375 nm depicting the electronic vibrations in this region which were further intensified signifying the uninterrupted PZO NFs synthesis. Final surface plasmon resonance induced by the mutual vibration of electrons, PZO NFs exhibited lambda maximum at 398 nm (Figure 2a). $Zn(NO_3)_2$ salt was reduced and stabilized in presence of *P. cerasifera* fruit extract without any addition of chemical reducing agents. Such reduction cum stabilization express the anti-oxidant power of phytochemicals found in *P. cerasifera* fruit extract. PZO NFs have diffraction peaks at 2θ values of 34.7°, 35.6°, 48°, 55.21°, 61° and 68°, which can be credited to (002), (012), (110), (013) and (201), respectively. Comparison with JCPDS card no. 36-1451 and peaks confirmed the single phase hexagonal (Wurtzite structure) for PZO NFs (Figure 2b). Crystalline nature of PZO NFs confirms the validity of pomosynthetic route as green and efficient method for getting nano ZnO. Furthermore, the average crystallite size pf PZO NF was determined to be 4.93 nm from Scherrer equation:

$$D=[K\lambda/\ \beta \cos\theta] \times Å \quad (3)$$

where, D is representing the average of crystal size in Å, K (0.9) is shape factor, λ is wavelength of X-ray Cu K_α (1.5406 Å) radiation, θ is the Bragg angle and β is the corrected line expressing NPs broadening.

FTIR analysis was done to comprehend the involvement of functional groups involved in stabilization and

Table 1: Functional groups detected in *P. cerasifera* fruit extract and PZO NFs calcined at 200 and 400°C.

FTIR peaks (cm^{-1})	Bond	Functional groups
P. cerasifera fruit powder		
3343	O–H stretch, H–bonded	Alcohol, phenol
2930	O-H Stretch	Carboxylic acid
1732	C=O Stretch	Ketones
1628	N-H Stretch	Amines
1400	C-C stretch	Aromatics
1261	C–N stretch	Aromatic amines
1078	C–N stretch	Aliphatic amines
891	C-C stretch	Aromatics
800	C–Cl stretch	Alkyl halides
744	C–Cl stretch	Alkyl halides
611	–C≡C–H: C–H bend	Alkynes
PZO NFs (calcined at 200°C)		
3484	O–H stretch, H–bonded	Alcohol, phenol
2851	C-H stretch	Alkanes
2101	–C≡C–	Alkynes
1244	C–N stretch	Aliphatic amines
835	C–Cl stretch	Alkyl halides
802	C–Cl stretch	Alkyl halides
725	C-H rock	Alkanes
638	C-Br	Alkyl halides
PZO NFs (calcined at 400°C)		
3507	O–H stretch, H–bonded	Alcohol, phenol
3404	O–H stretch, H–bonded	Alcohol, phenol
2851	C-H stretch	Alkanes
2764	H–C=O: C–H stretch	Aldehydes
1325	C–N stretch	Aromatic amines
1117	C–N stretch	Aliphatic amines
835	C–Cl stretch	Alkyl halides
725	C–H rock	Alkanes
629	–C≡C–H: C–H bend	Alkynes

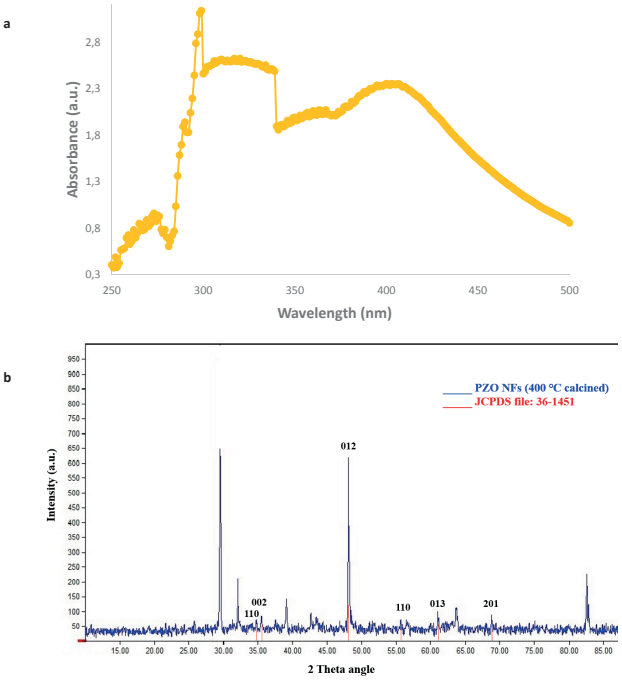

Figure 2: a) UV-Vis spectrum, b) XRD pattern of ZnO nano falcate.

reduction of PZO NFs by *P. cerasifera* fruit extract (Figure 3 a,b). FTIR spectra was recorded between the wavenumber spanning over a range of 4000–400 cm^{-1}. FTIR spectra of *P. cerasifera* fruit extract confirmed the presence of O–H stretching with absorption bands at 3343 and 2930 cm^{-1} signifying polyols in it. Broad peaks at 1732 and 1628 cm^{-1} represents C=O and N-H of ketones and amines respectively. Relatively smaller and broader peaks at 1400, 1261 and 1078 cm^{-1} of C-C, C-N and C-N stretch represents the presence of aromatics, aromatic amines and aliphatic amines. Detected bands signify different types of polyols i.e. phenols and flavonoids, proteinaceous and terpenoids profusion in P. *cerasifera* fruit extract. FTIR spectra for PZO NFs synthesized at different calcination temperatures expressed the loss of few peaks and emergence of new peaks when reduced and stabilized by *P. cerasifera* fruit extract. PZO NFs (200°C) have shown absorption bands around 3484, 2851, 2101, 1244 and 835 cm^{-1} of alcohol/phenols, alkanes, alkynes, aliphatic amines and alkyl halides. PZO NFs (400°C) expressed variance in absorption bands due to better conversion into PZO NFs at elevated temperatures with 3507, 3404, 2851, 2764 and 1325 cm^{-1} of O–H, C-H, H–C=O, C–H and C–N stretching mode. Phenolic compounds in P. *cerasifera* fruit extract interact with PZO NPs during reduction and stabilization and induce transmittance shifts.

PZO NFs were analyzed for surface morphology and size ranges by scanning electron microscopy (SEM JOEL JSM-6490, Germany). PZO NFs were highly influenced by variation in calcination temperatures. Nearly smooth surface morphology with larger sized nano falcates in range of 72.11 -120.00 nm were detected for PZO NPs calcined at 200°C. Figure 4 (a-e) shows nano falcate of sickle like hooked shape nano ZnO at different resolutions. PZO NFs calcined at 400°C (Figure 4 f-j) expressed rough surface morphology [28] with roughly nano falcates in protrusion like network with irregular orientations. Nano-falcates obtained at 400°C were not evenly distributed like that of 200°C but has an alleviated size ranges of 56.57-107.70 nm thus revealing the sensitivity of ZnO nano falcates towards calcination temperatures. Topographical and surface roughness of nano falcates was analyzed via atomic force microscopy. AFM was conducted on variable

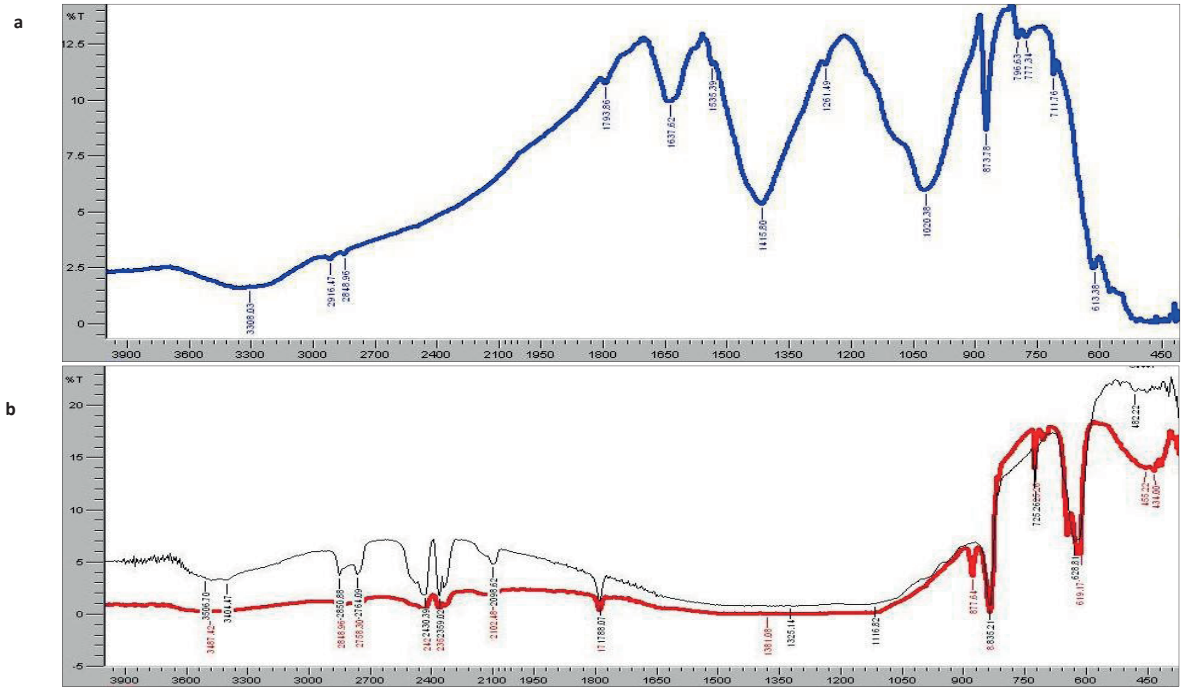

Figure 3: a) FTIR spectrum *P. cerasifera* fruit extract and b) FTIR spectra overlay of *P. cerasifera* fruit extract mediated ZnO nano falcate calcined at 200 and 400°C.

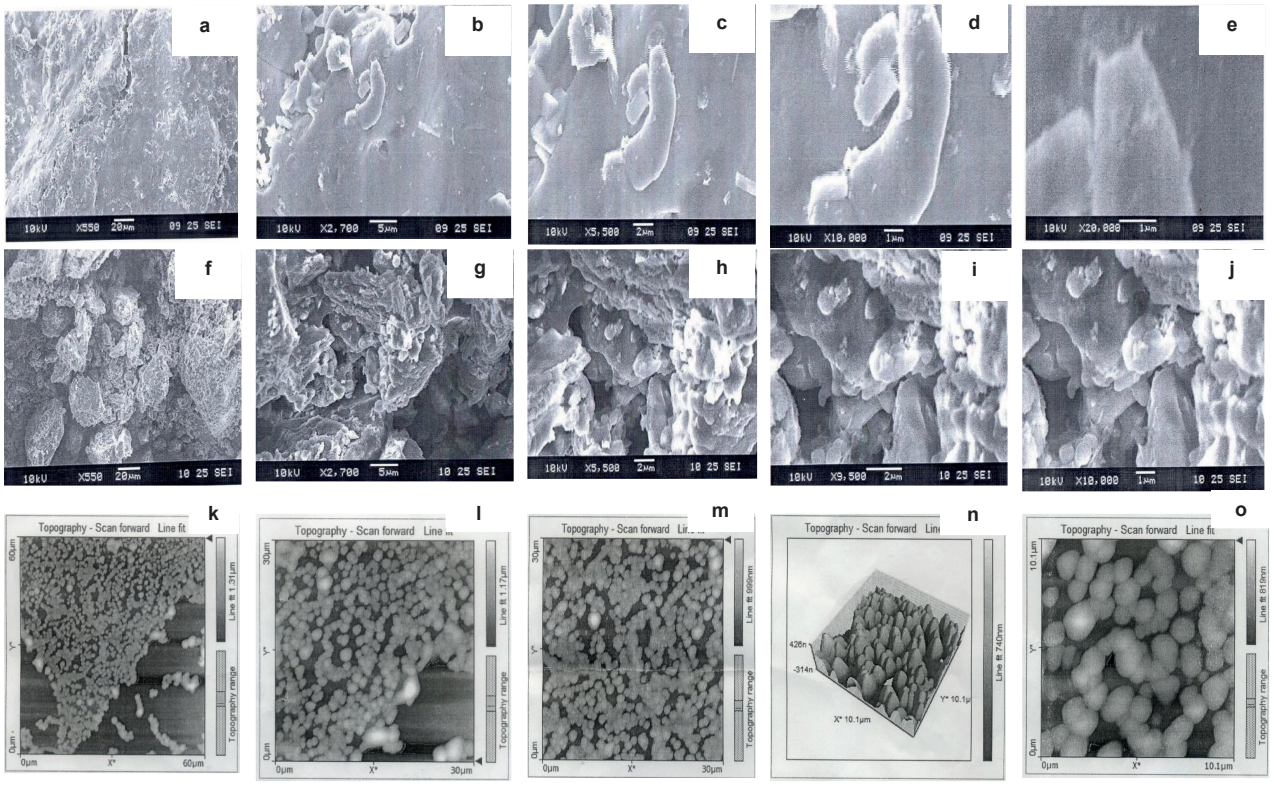

Figure 4: Scanning electron micrographs, a-e) *P. cerasifera* mediated ZnO nano falcate calcined at 200°C, f-j) *P. cerasifera* mediated ZnO nano falcate calcined at 400°C, k-o) Atomic force micrographs of *P. cerasifera* mediated ZnO nano falcate in 2D and 3D structures.

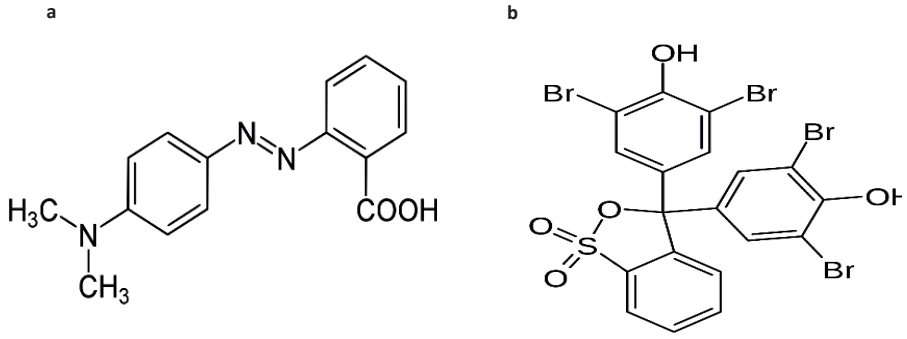

Figure 5: Chemical structures of target dyes a) methyl red and b) bromophenol blue.

magnification ranges (Figure 4k-o). 2D and 3D micrographs show the smooth nano falcates stabilized and caped by phytoconstituents of *P. cerasifera* fruit extract. AFM revealed the polydispersity and slightly elongated shapes of nano falcates.

3.3 Photocatalytic activity of PZO NFs

Dyes have been known as the environmental pollutants since they have very good solubility in water thus rendering it unsuitable for consumption by human and other organisms. In many cases dyes become persistent organic pollutants. Consequently, efforts have been done for the pretreatment of dyes particularly in textile industry. Removal of these dyes through physicochemical or radiation reduction is associated with release of even more toxic degradation products thus challenging the credibility of these processes. Thus, the environmental integrity is further deteriorated instead of betterment [29]. Photocatalytic phenomenon is governed by photons that possess harmonious behavior or surpass the band gap energy of semiconductor of interest [30]. The conversion of persistent organic pollutants to harmless products via photocatalytic pathway in case of metal oxides is mainly dependent upon the incidence of light radiations. Such radiations are taken up by the metal oxides for excitation of electrons from valence to conduction band. The consequent hole developed in valence band is then associated with generation of radicals after absorption of electron. Dyes are oxidized to their leuco forms (achromatic form) by the previously generated radicals signifying the conversion of environmentally perilous dyes to benign components [31]. ZnO has been utilized for photocatalytic degradation of chemicals due to its elevated activity in UV region [32]. Ecologically toxic pollutants have been efficiently degraded with ZnO owing to its innocuous nature, economic favorability and augmented photo degradative potential [33].

Methyl red and bromophenol blue are heterocyclic aromatic dyes (Figure 5a,b). Degradation of these dyes was studied in absence and presence of PZO NFs with direct exposure to solar irradiance. (Figure 6a,b). Dye reference solutions without PZO NFs remained unaffected by solar irradiance. Photocatalytic dye degradation for both dyes was monitored via alleviating UV-Vis absorption peaks. Upon addition of PZO NFs, the degradation was completed in less than an hour with complete color disappearance signifying the remarkable photocatalytic potential of PZO NFs. Methyl red, significant textile dye possessing the most reactive nature photo catalytically degraded by ZnO nanoparticles within 35min has also been reported [34]. Results revealed 96.77% of bromophenol blue in 50 minutes exceeded methyl red with 82.65% in degradation in same exposure time (Figure 6c). However, photo degradation with commercial ZnO has also exhibited discoloration extents up to 99% of MR producing no absorption peak. Such discoloration signifies the MR transformation to simpler organic form due to elimination of main chromophore azo group in aqueous solution [35]. Comparative analysis of ZnO with commercial as well as prepared ZnO NPs, the PZO NFs are good in terms of efficiency and handiness.

Variety of physicochemical methods i.e. absorptive [36], photocatalytic [37] and biological degradation [38] have been devised for conversion of highly toxic and persistent organic pollutant bromophenol blue. However, these technologies have not been successful so far due to their alleviated efficiency, higher cost and operational complications [39]. Thus, such challenges have been addressed and BB in the present research has been photodegraded with PZO NFs as photo catalysts in conformity with all principles of Green chemistry. Degradation percentages up to 84.2% in 30min [40], 95% in 90 min [41] and 64% in 160 min [42] have been achieved with ZnO photo catalysts suggestive of PZO NFs with 96.77% as exceedingly efficient over conventional

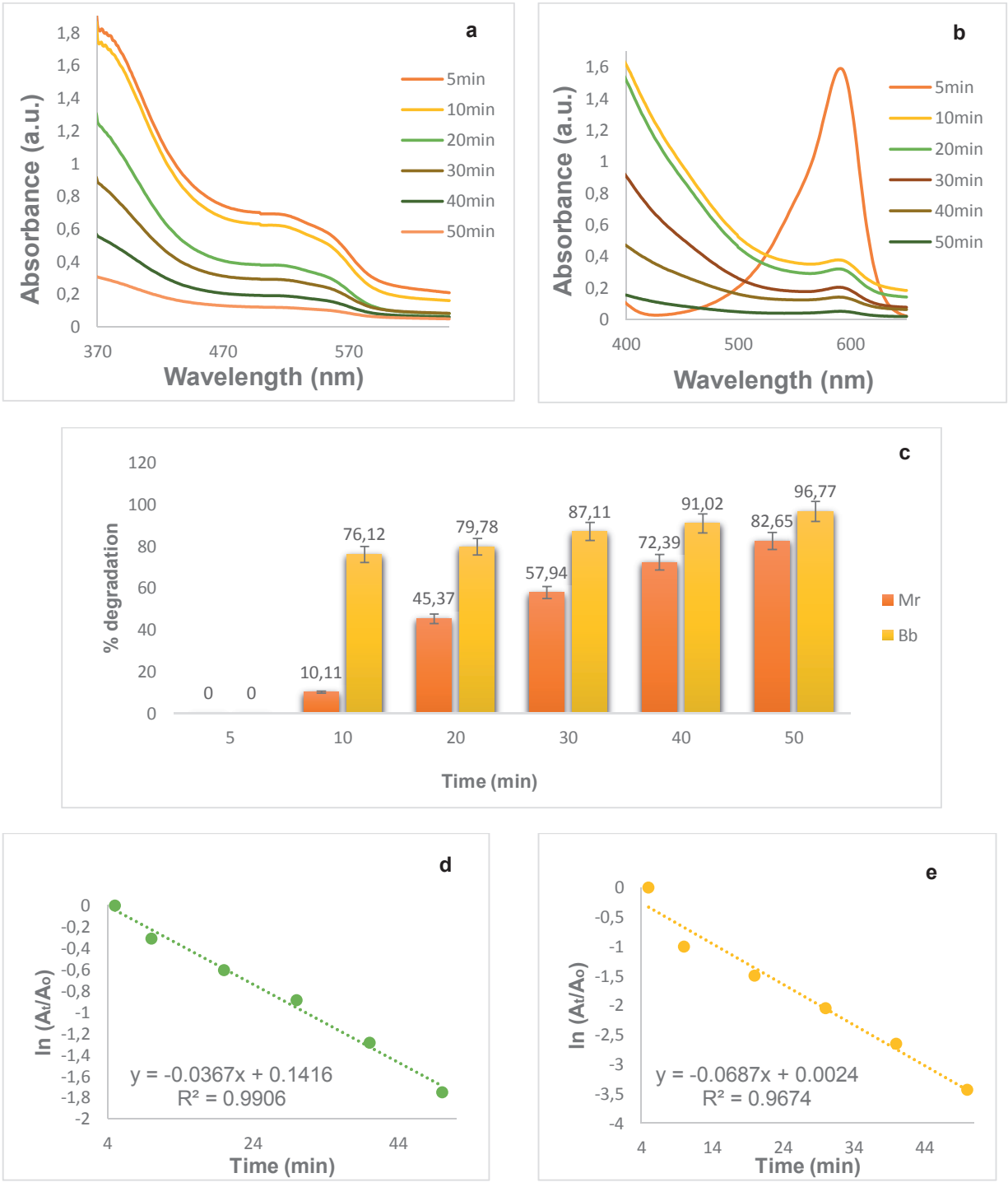

Figure 6: Alleviating UV-vis spectra expressing photocatalytic dye degradation potential of pomosynthetic ZnO nano falcates calcined at 400°C: a) methyl red, b) bromophenol blue, c) percent degradation, d) e) ln (A_t/A_o) *vs* time plot of methyl red and bromophenol blue.

ZnO NPs. Such photo degradation is governed by the coverage of the active sites of PZO NFs leaving only fewer photons reaching PZO NFs' surface. This can be attributed to the maximum light absorption by BB molecules instead of PZO NFs [41]. However, the competition between BB molecules and water molecules for photo commenced H^+ inducing a diminution sin OH● and other reactive species generation. PZO NFs excelled in photo degradation of BB due to stronger electrostatic forces in form of adsorptive interactions between cationic PZO NFs' surface and

Table 2: ***In vitro*** antibacterial and antifungal efficacy of pomosynthesized ZnO nano falcate against plant phytopathogens.

Bacterial Strain	Salt sol. (10 µL)	Standard* (10 µL)	PCFE (10 µL)	PZO NFs (2 µL)	PZO NFs (4 µL)	PZO NFs (6 µL)	PZO NFs (10 µL)
X. citri	0	14.03±0.05	12.03±0.06	6.03±0.06	7.03±0.06	10.30±0.15	14.10±0.10
P. syringae	0	18.07±0.12	6.07±0.03	8.10±0.08	11.20±0.01	16.10±0.10	19.03±0.06
Fungal cultures	Salt sol. (10 µL)	Standard** (10 µL)	PCFE (10 µL)	PZO NFs (5 µL)	PZO NFs (10 µL)	PZO NFs (15 µL)	PZO NFs (20 µL)
A. niger	0	18.02±0.02	12.02±0.01	10.04±0.02	12.05±0.03	14.02±0.02	17.07±0.02
A. flavus	0	25.09±0.01	13.11±0.08	9.05±0.03	13.06±0.03	17.05±0.02	20.05±0.03
A. fumigatus	0	16.08±0.09	6.01±0.01	4.08±0.2	8.01±0.01	12.04±0.02	18.05±0.04
A. terreus	0	13.21±0.00	8.03±0.02	5.04±0.03	8.03±0.04	12.38±0.10	15.01±0.01
P. chrysogenum	0	23.06±0.03	6.02±0.01	4.07±0.02	8.02±0.02	16.09±0.01	22.07±0.02
F. solani	0	18.06±0.08	9.01±0.01	7.05±0.02	11.05±0.03	16.03±0.04	21.01±0.04
L. theobromae	0	19.08±0.05	11.04±0.02	10.02±0.01	14.04±0.04	18.05±0.03	24.02±0.01

* *Ampicillin.* ** *Amphotericin B.*

anionic dye solution [43]. Figure 6 d,e illustrated the reaction kinetics (ln (A_t/A_o) vs time for determining the order of photocatalytic reaction. The reduction caused by PZO NFs was found to be pseudo first order kinetics. There was a linear relationship between ln (A_t/A_o) vs time with R^2= 0.99 and 0.96 for methyl red and bromophenol blue respectively. Thus PZO NFs synthesized via green route were revealed to be efficient candidates for nano bioremediation at low cost and easy mode of synthesis.

3.4 Antimicrobial efficacy

Nanoscale ZnO particles have been significantly employed for bacterial inhibition at a global scale due to advances in nanotechnology [44]. Though, ZnO nanoparticles based bacterial inhibition has been rigorously studied, despite this fact the accurate toxicological mechanism is yet contentious and needs thorough investigations for polemical mechanisms given so far. PZO NFs in this regard have not been reported for the tested strains. Thus, present study is the first investigation of *P. cerasifera* fruit mediated ZnO NFs' potency against pathogenic bacterial and fungal strains. PZO NFs were evaluated for their bacterial and fungicidal efficacy via by standard Kirby–Bauer disc diffusion assay and the microbial growth prevention was quantified from the zone of inhibition (ZOI) in mm. PZO NFs were loaded on discs in dose dependent manner with 2, 4, 6 and 10 µL (Table 2). Dose dependent *in vitro* antibacterial assay of PZO NFs exhibited elevated activities against plant pathogens i.e., *X. citri* and *P. syringae* in comparison to the standard drug. *P. cerasifera* fruit extract produced commendable zone of 12.03 mm in comparison to 14.03 mm produced by standard drug. Thus showing the bioprospects of *P. cerasifera* fruit extract against *X. citri*, however the clearance zone for the later strain was smaller comparatively. Overall PZO NFs inhibited the growth of all nine microbes with higher clearance zones against bacterial strains, such obliterative mechanism can be due to PZO NFs direct interaction with bacterial cell walls and ultimate destruction of cellular entirety [45-48] in addition to the generation of inhibitory Zn^{2+} ions ions [49,50] and ROS generation [51]. Augmented growth clearance zones against two bacterial strains expresses the PZO NFs potential in inhibition as well as the bacterial strains' susceptibility towards PZO NFs [52-54]. Due to thinner cell walls found in all Gram negative bacteria which is easily susceptible to the facile rupture and quicker assimilation. The concentration of PZO NFs expressed a positive correlation with inhibition and the highest concentration exceeded the standard drug in inhibiting both pathogenic strains [55,56]. Such an enhanced antibacterial potency of PZO NFs significantly portrays the higher susceptibility of test microbes and decreased resistance thus favoring the development of synthesized PZO NFs into bactericidal agents on commercial scale. PZO NFs utilization for agricultural biocidal and biomedical purpose is advantageous over commercially available ZnO antibacterial agents because they exhibit no toxicity at lower concentrations to human cells but possess higher toxicities against bacterial strains [57]. In case of human disease, ZnO has been shown to provide protection against *E. coli* induced intestinal ailments by inhibition of *E. coli* adhesion and internal residence [58]. ZnO NPs have succeeded in reducing up to 99% of bacterial growth [59].

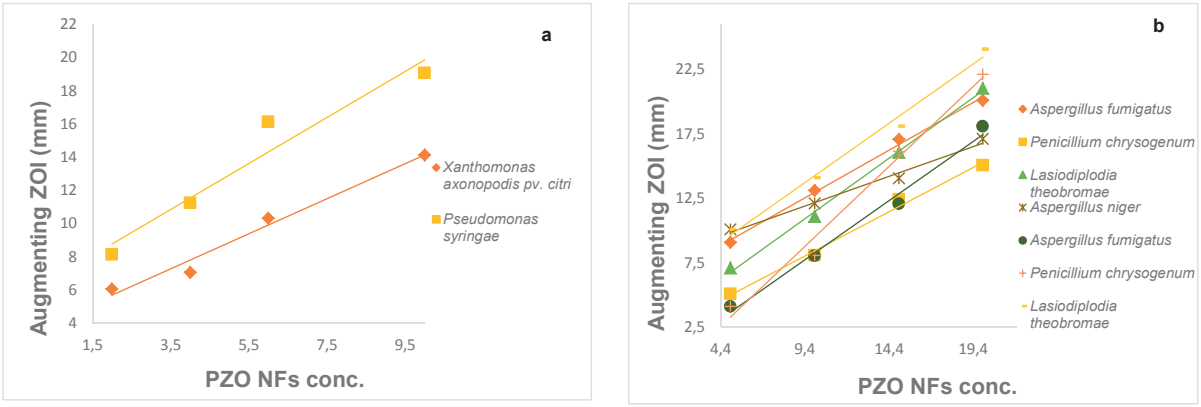

Figure 7: Comparative *in vitro* antimicrobial efficacy of pomosynthetic ZnO nano falcates derived from *P. cerasifera* calcined at 400°C against a) bacterial and b) fungal pathogens.

PZO NFs loaded discs in dose dependent manner revealed variable and higher zones of inhibitions for all fungal pathogens i.e. *A. niger, A. flavus, A. fumigatus, A. terreus, P. chrysogenum, F. solani* and *L. theobromae*. The results obtained for PZO NFs' highest dose are comparable with those of the standard drug. For all the pathogenic fungal cultures, *P. cerasifera* fruit extract shown enhanced antifungal activity (Table 2). The dose dependent *in vitro* assay expressed highest inhibition against *L. theobromae* (24.02 mm) and lowest against *A. terreus* (15.01 mm) (Figure 7a). Linear relationship between PZO NFs concentration and antifungal activity enhancement can be attributed to the consequent incremental ROS production as reported earlier [60-62]. Toxicological pattern of PZO NFs against targeted strains may vary depending upon various factors in addition to the morphological and size ranges of PZO NFs. PZO NFs with hexagonal (Wurtzite structure) crystals contained edges and corners as reactive surfaces [63, 64]. Defect sites are known for their elevated reactivity and catalysis of ROS production that directly increases the antimicrobial activity [65]. PZO NFs antifungal activity is in agreement with reported studies on different fungal strains; however, seven fungal strains tested with PZO NFs have never been reported before. ZnO NPs synthesized via myriad of synthetic routes has been employed for inhibition of *A. flavus*, *A. fumigatus* and *A. niger* but no reports have been found on *Prunus cerasifera* mediated PZO NFs. Thus, PZO NFs can effectively control the harmful fungal strains and can be used for agricultural and biomedical purposes [66].

Metallic nanoparticles have been investigated against a wide range of microbes but data on ZnO nanomaterials as antifungal agents against agricultural pests is scanty. Higher food spoilage induced by fungal species on global scale is not only an economical but environmental concern, for which green antifungal treatments needs to be developed [67]. Targeted fungal strains are not only phytopathogenic in nature but also source of human ailments e.g., *A. fumigatus* can cause hypersensitivity pneumonitis and *A. terreus* causes invasive aspergillosis. Thus, PZO NFs' antifungal potential against these pathogens offers facile, biomimetic and inexpensive treatment. Though deeper insights are required for comprehension of accurate antifungal mechanism of PZO NFs, but based upon similar reports on ZnO NPs, it is assumed that PZO NFs interact with fungal cell inducing structural deformation and interfering with the cellular functionalities [68]. Thus, such distortions ultimately results into fungal cell death signifying the antifungal potential of PZO NFs [69]. Synthetic route and conditions needs to be kept uniform for ensuring the antifungal activity of PZO NFs [70]. Comparatively higher fungicidal activity in terms of ZOI was obtained due to the bioreduction of PZO NFs with *P. cerasifera* fruit phytoconstituents which not only bio-capped the PZO NFs but also stabilized them for longer durations. Such remarkable inhibition by PZO NFs makes them suitable choice for biomedical and agricultural treatments [71]. *P. cerasifera* fruit mediated metallic nanoparticles in addition to PZO NFs have been found effective against variety of microorganisms [72] thus minimizing the need for bactericides and fungicides with reported toxicities and harmful impacts on environment [73,74].

4 Conclusion

Plants being the natural reservoirs of chemicals, can be used for development of advanced nanoscale materials through biomimetic routes. Facile, unprecedented and

nontoxic method was adopted for fabrication of zinc oxide nano falcates from reducing agents of *P. cerasifera* pomological extract. Fabrication and stabilization of zinc oxide nano falcates is attributed to the phenols and amines abundantly present in *P. cerasifera*. Zinc oxide nano falcates of wurtzite structure has lambda maximum at 398 nm. Zinc oxide nano falcates exhibited 4.93 nm average crystallite size. Methyl red and bromophenol blue were efficiently degraded with zinc oxide nano falcates i.e., 82.65 and 96.77% in 50 min. Zinc oxide nano falcates are effective against the tested bacterial and fungal strains with zone of inhibitions as high as 24 mm. *P. cerasifera* fabricated zinc oxide nano falcates are expected to be of extensive applications in remediation of chemicals and plant protection against pathogens.

Acknowledgments: Authors are grateful to Fatima Jinnah Women University, Rawalpindi, Pakistan for provisioning of all required chemicals and analytical facilities.

Conflict of interest: Authors state no conflict of interest.

References

[1] Chen J.C., Tang C.T., Preparation and application of granular ZnO/Al_2O_3 catalyst for the removal of hazardous trichloroethylene. J. Hazard Mater. 2007, 142, 88-96.

[2] Jayaseelan C., Rahuman A.A., Kirthi A.V., Marimuthu S., Santhoshkumar T., Bagavan A., Rao K.B., Novel microbial route to synthesize ZnO nanoparticles using *Aeromonas hydrophila* and their activity against pathogenic bacteria and fungi. Spectrochim Acta Mol. Biomol. Spectrosc., 2012, 90, 78-84.

[3] Priyadharshini R.I., Prasannaraj G., Geetha N., Venkatachalam P., Microwave-mediated extracellular synthesis of metallic silver and zinc oxide nanoparticles using macro-algae (*Gracilaria edulis*) extracts and its anticancer activity against human PC3 cell lines. Biotechnol. App.l Biochem., 2014, 174, 2777-2790.

[4] Sharma D., Sabela M.I., Kanchi S., Mdluli P.S., Singh G., Stenström T.A., et al., Biosynthesis of ZnO nanoparticles using *Jacaranda mimosifolia* flowers extract: Synergistic antibacterial activity and molecular simulated facet specific adsorption studies. J. Photochem Photobiol., 2016, 162, 199-207.

[5] Siripireddy B., Mandal B.K., Facile green synthesis of zinc oxide nanoparticles by *Eucalyptus globulus* and their photocatalytic and antioxidant activity. Adv. Powder Technol., 2017, 28, 785-797.

[6] Stan M., Popa A., Toloman D., Dehelean A., Lung I., Katona G., Enhanced photocatalytic degradation properties of zinc oxide nanoparticles synthesized by using plant extracts. Mater. Sci. Semicond. Process., 2015, 39, 23-29.

[7] Birwal P., Deshmukh G., Saurabh S.P., Plums: A Brief Introduction. J. Food Nutr. Popul. Health., 2017, 1, 1-5.

[8] Wang Y., Chen X., Zhang Y., Chen X., Antioxidant activities and major anthocyanins of myrobalan plum (*Prunus cerasifera* Ehrh.). J. Food Sci., 2012, 77, 1-6.

[9] Ştefănuţ M.N., Căta A., Ienaşcu I., Comparative Antioxidant Activity Of Some *Prunus* Genus Fruits. Rev. Roum. Chim., 2015, 60, 603-608.

[10] Jingru Z., Sun H., Zhicheng L., Haifei L., Jing L., Kun W., Analysis of Fruit Polyphenols diversity of wild cherry plum (*Prunus cerasifera*). Fruit Sci., 2012, 34, 567-575.

[11] Ramesh M., Anbuvannan M., Viruthagiri G., Green synthesis of ZnO nanoparticles using *Solanum nigrum* leaf extract and their antibacterial activity. Spectrochim. Acta Mol. Biomol. Spectrosc., 2015, 136, 864-870.

[12] Elavarasan N., Kokila K., Inbasekar G., Sujatha V., Evaluation of photocatalytic activity, antibacterial and cytotoxic effects of green synthesized ZnO nanoparticles by *Sechium edule* leaf extract. Res. Chem. Intermed., 2017, 43, 3361-3376.

[13] Srikar S.K., Giri D.D., Pal D.B., Mishra P. K., Upadhyay S.N., Light induced green synthesis of silver nanoparticles using aqueous extract of *Prunus amygdalus*. Green Sustain. Chem., 2016, 6, 26-33.

[14] Iqbal J., Amin M., Shahid M., Islam N.U., Amin R., Zaib S., A multi-target therapeutic potential of *Prunus domestica* gum stabilized nanoparticles exhibited prospective anticancer, antibacterial, urease-inhibition, anti-inflammatory and analgesic properties. BMC Complement Altern. Med., 2017, 17, 2-17.

[15] Kumar R., Ghoshal G., Jain A., Goyal M., Rapid green synthesis of silver nanoparticles (Ag NPs) using (*Prunus persica*) plants extract: exploring its antimicrobial and catalytic activities. J. Nanomed Nanotechnol., 2017, 8, 2-8.

[16] Kumar B., Angulo Y., Smita K., Cumbal L., Debut A., Capuli cherry-mediated green synthesis of silver nanoparticles under white solar and blue LED light. Particuology., 24, 2016, 123-128.

[17] Dauthal P., Mukhopadhyay M., *In-vitro* free radical scavenging activity of biosynthesized gold and silver nanoparticles using *Prunus armeniaca* (apricot) fruit extract. J. Nanopart. Res., 2013, 15, 2-11.

[18] Manikandan V., Velmurugan P., Park J.H., Lovanh N., Seo S.K., Jayanthi P., Oh B.T., Synthesis and antimicrobial activity of palladium nanoparticles from *Prunus × yedoensis* leaf extract. Mater Lett., 2016, 185, 335-338.

[19] Kargar M., Reza M., Shafiee M., Ghashang M., Green protocol preparation of ZnO nanoparticles in *Prunus cerasus* juice media. Nanosci Nanotech-Asia., 2015, 5, 44-49.

[20] Kırbağ S., Göztok F., Antioxidant and antimicrobial activity of *Prunus cerasifera* cv. '' Pissardii Nigra. Artvin Çoruh Üniversitesi Orman Fakültesi Dergisi., 2016, 17, 106-111.

[21] Ajaib M., Haider S.K., Zikrea A., Siddiqui M.F., Ethnobotanical studies of shrubs and trees of Agra Valley Parachinar, Upper Kurram Agency, Pakistan. FUUAST J Bio., 2014, 4, 73-81.

[22] Song W., Qin S.T., Fang F.X., Gao Z.J., Liang D.D., Liu L.L., Yang H.B., Isolation and purification of condensed tannin from the leaves and branches of *Prunus cerasifera* and its structure and bioactivities. Biotechnol. Appl. Biochem., 2017, 1-12. https://doi.org/10.1007/s12010-017-2635-9.

[23] Horvath A., Balsemin E., Barbot J. C., Christmann H., Manzano G., Reynet P., Mariette S., Phenotypic variability and genetic structure in plum (*Prunus domestica* L.), cherry plum (*P.*

cerasifera Ehrh.) and sloe (*P. spinosa* L.). Sci. Hort., 2011, 129, 283-293.
[24] Stacewicz-Sapuntzakis M., Bowen P.E., Hussain E.A., Damayanti-Wood B.I., Farnsworth N.R., Chemical composition and potential health effects of prunes: a functional food? Crit. Rev. Food Sci. Nutr., 2001, 41, 251-286.
[25] Gündüz K., Saraçoğlu O., Variation in total phenolic content and antioxidant activity of *Prunus cerasifera* Ehrh. selections from Mediterranean region of Turkey. Sci. Hort., 2012, 134, 88-92.
[26] Barrett A.H., Farhadi N.F., Smith T.J., Slowing starch digestion and inhibiting digestive enzyme activity using plant flavanols/tannins—a review of efficacy and mechanisms. LWT-Food Sci. Tech.. 2018, 394-399. https://doi.org/10.1016/j.lwt.2017.09.002.
[27] Kato C.G., Gonçalves G.D.A., Peralta R.A., Seixas F.A.V., deSá-Nakanishi A.B., Bracht L., Peralta R.M., Inhibition of α-Amylases by condensed and hydrolysable tannins: focus on kinetics and hypoglycemic actions. Enzyme Res., 2017, 1-12. https://doi.org/10.1155/2017/5724902.
[28] 28-Sisubalan N., Ramkumar V.S., Pugazhendhi A., Karthikeyan C., Indira K., Gopinath K., Basha M.H.G., ROS-mediated cytotoxic activity of ZnO and CeO_2 nanoparticles synthesized using the *Rubia cordifolia* L. leaf extract on MG-63 human osteosarcoma cell lines. Environ. Sci. Pollut. Res., 2017, 1-11. https://doi.org/10.1007/s11356-017-0003-5.
[29] Dutta A.K., Maji S.K., Adhikary B., γ-Fe_2O_3 nanoparticles: an easily recoverable effective photo-catalyst for the degradation of rose bengal and methylene blue dyes in the waste-water treatment plant. Mater. Res. Bull., 2014, 49, 28-34.
[30] Saleh T.A., Gupta V.K., Photo-catalyzed degradation of hazardous dye methyl orange by use of a composite catalyst consisting of multi-walled carbon nanotubes and titanium dioxide. J. Colloid Interface Sci., 2012, 371, 101-106.
[31] Vidya C., Prabha M.C., Raj M.A., Green mediated synthesis of zinc oxide nanoparticles for the photocatalytic degradation of Rose Bengal dye. Envir Nanotech Mon Manage., 2016, 6, 134-138.
[32] Quintana M., Ricra E., Rodrıguez J., Estrada W., Spray pyrolysis deposited zinc oxide films for photo-electrocatalytic degradation of methyl orange: influence of the pH. Catal Today., 2002, 76, 141-148.
[33] Saad S.R., Mahmed N., Abdullah M.M.A.B., Sandu A.V., Self-cleaning technology in fabric: A review. In IOP: Mater. Sci. Eng., 2016, 133, 1-9.
[34] Davar F., Majedi A., Mirzaei A., Green synthesis of ZnO nanoparticles and its application in the degradation of some dyes. J. Am. Ceram. Soc., 2015, 98, 1739-1746.
[35] Singh N.K., Saha, S., Pal A., Methyl red degradation under UV illumination and catalytic action of commercial ZnO: a parametric study. Desalin Water Treat., 2015, 56, 1066-1076.
[36] Salem A.I., Kinetics of the oxidative color removal and degradation of bromophenol blue with hydrogen peroxide catalyzed by copper (II)-supported alumina and zirconia. Appl Catal. B. Environ., 2000, 28, 153-162.
[37] Bouanimba N., Zouaghi R., Laid N., Sehili T., Factors influencing the photocatalytic decolorization of Bromophenol blue in aqueous solution with different types of TiO_2 as photocatalysts. Desalination., 2011, 275, 224-230.
[38] Ghaedi M., Ghaedi A.M., Negintaji E., Ansari A., Vafaei A., Rajabi M., Random forest model for removal of bromophenol blue using activated carbon obtained from *Astragalus bisulcatus* tree. Ind. Eng. Chem. Res., 2014, 20, 1793-1803.
[39] Zhang C., Wang J., Zhou H., Fu D., Gu Z., Anodic treatment of acrylic fiber manufacturing wastewater with boron-doped diamond electrode: a statistical approach. Chem. Eng. J., 2010, 161, 93-98.
[40] Sanjay S.S., Yadav R.S., Pandey A.C., Synthesis of lamellar porous photocatalytic nano ZnO with the help of anionic surfactant. Adv. Mater. Lett., 2013, 4, 378-384.
[41] Samar M.M.E., Photocatalytic Degradation of Organic Compounds in Water using Nanoparticulate Thin Film, Al-Azhar University –Gaza, 2015.
[42] Aby H., Kshirsagar A., Khanna P.K., Plasmon mediated photocatalysis by solar active Ag/ZnO nanostructures: degradation of organic pollutants in aqueous conditions. J. Mater. Sci. Nanotechnol., 2016, 4, 103, 1-14.
[43] Mashkour M.S., Decolorization of bromophenolblue dye under uv-radiation with ZnO as catalyst. Iraqi Nat. Chem., 2012, 46, 189-198.
[44] Sirelkhatim A., Mahmud S., Seeni A., Kaus N.H.M., Ann L.C., Bakhori S.K.M., Mohamad D., Review on zinc oxide nanoparticles: antibacterial activity and toxicity mechanism. Nano-Micro Lett., 2015, 7, 219-242.
[45] Brayner R., Ferrari-Iliou R., Brivois N., Djediat S., Benedetti M.F., Fiévet F., Toxicological impact studies based on *Escherichia coli* bacteria in ultrafine ZnO nanoparticles colloidal medium. Nano Lett., 2006, 6, 866-870.
[46] Zhang C., Wang J., Zhou H., Fu D., Gu Z., Anodic treatment of acrylic fiber manufacturing wastewater with boron-doped diamond electrode: a statistical approach. Chem. Eng. J., 2010, 161, 93-98.
[47] Adams L.K., Lyon D.Y., Alvarez P.J., Comparative eco-toxicity of nanoscale TiO_2, SiO_2, and ZnO water suspensions. Water Res., 2006, 40, 3527-3532.
[48] Applerot G., Lipovsky A., Dror R., Perkas N., Nitzan Y., Lubart R.,Gedanken A. Enhanced antibacterial activity of nanocrystalline ZnO due to increased ROS-mediated cell injury. Adv. Funct. Mater., 2009, 19, 842-852.
[49] Kasemets K., Ivask A., Dubourguier H.C., Kahru A., Toxicity of nanoparticles of ZnO, CuO and TiO_2 to yeast *Saccharomyces cerevisiae*. Toxico In Vitro., 2009, 23, 1116-1122.
[50] Li M., Zhu L., Lin D., Toxicity of ZnO nanoparticles to *Escherichia coli*: mechanism and the influence of medium components. Envir. Sci. Tech., 2011, 45, 1977-1983.
[51] Jalal R., Goharshadi E.K., Abareshi M., Moosavi M., Yousefi A., Nancarrow P., ZnO nanofluids: green synthesis, characterization, and antibacterial activity. Mater Chem Phy., 2010, 121, 198-201.
[52] Ananth A., Dharaneedharan S., Seo H.J., Heo M.S., Boo J.H., Soft jet plasma-assisted synthesis of Zinc oxide nanomaterials: Morphology controls and antibacterial activity of ZnO. Chem Eng J., 2017, 322, 742-751.
[53] Parthasarathy G., Saroja M., Venkatachalam M., Evanjelene V.K., Characterization and antibacterial activity of green synthesized ZnO nanoparticles from *Ocimum basilicum* leaf extract. Adv. Biores., 2017, 8, 29-35.
[54] Ba-Abbad M.M., Takriff M.S., Benamor A., Mahmoudi E., Mohammad A.W., Arabic gum as green agent for ZnO

nanoparticles synthesis: properties, mechanism and antibacterial activity. J. Mater. Sci. Mater. Electron., 2017, 1-8. https://doi.org/10.1007/s10854-017-7023-2.
[55] Farzana R., Iqra P., Shafaq F., Sumaira S., Zakia K., Hunaiza T., Husna M., Antimicrobial Behavior of Zinc Oxide Nanoparticles and β-Lactam Antibiotics against Pathogenic Bacteria. Arch Clinical Microbio., 2017, 8, 1-5.
[56] Ghidan A.Y., Al-Antary T.M., Salem N.M., Awwad A.M., Facile green synthetic route to the zinc oxide (ZnO NPs) nanoparticles: effect on green peach aphid and antibacterial activity. J. Agri. Sci., 2017, 9, 131-138.
[57] Padmavathy N., Vijayaraghavan R., Enhanced bioactivity of ZnO nanoparticles—an antimicrobial study. Sci. Tech. Adv. Mater., 2008, 9, 1-7.
[58] Roselli M., Finamore A., Garaguso I., Britti M.S., Mengheri E., Zinc oxide protects cultured enterocytes from the damage induced by *Escherichia coli*. J Nutri., 2003, 133, 4077-4082.
[59] Jones N., Ray B., Ranjit K.T., Manna A.C., Antibacterial activity of ZnO nanoparticle suspensions on a broad spectrum of microorganisms. FEMS Microbiol Lett., 2008, 279, 71-76.
[60] Raghupathi K.R.; Koodali R.T.; Manna A.C., Size-dependent bacterial growth inhibition and mechanism of antibacterial activity of zinc oxide nanoparticles. Langmuir., 2011, 27, 4020-4028.
[61] Sonia S., Ruckmani K., Sivakumar M., Antimicrobial and antioxidant potentials of biosynthesized colloidal zinc oxide nanoparticles for a fortified cold cream formulation: A potent nanocosmeceutical application. Mater .Sci. Eng. C., 2017, 79, 581-589.
[62] Khalil A.T., Ovais M., Ullah I., Ali M., Shinwari Z.K., Khamlich S., Maaza M., *Sageretia thea* (Osbeck.) mediated synthesis of zinc oxide nanoparticles and its biological applications. Nanomedicine., 2017, 12, 1767-1789.
[63] Stankic S.; Suman S.; Haque F.; Vidic J., Pure and multi metal oxide nanoparticles: synthesis, antibacterial and citotoxic properties. J. Nanobiotech., 2016, 14, 2-20.
[64] Lakshmi P.V.; Vijayaraghavan R., Insight into the mechanism of antibacterial activity of ZnO: surface defects mediated reactive oxygen species even in the dark. Langmuir., 2015, 31, 9155-9162.
[65] Sierra-Fernandez A., De la Rosa-García S.C., Gomez-Villalba L.S., Gómez-Cornelio S., Rabanal M.E., Fort R., Quintana P., Synthesis, photocatalytic, and antifungal properties of MgO, ZnO and Zn/Mg oxide nanoparticles for the protection of calcareous stone heritage. ACS Appl. Mater. Interfaces., 2017, 9, 24873-24886.
[66] Auyeung A., Casillas-Santana M.Á., Martínez-Castañón G.A., Slavin Y.N., Zhao W., Asnis J., Bach H., Effective Control of Molds Using a Combination of Nanoparticles. PloS one., 2017, 12, 1-13.
[67] Sardella D., Gatt R., Valdramidis V.P., Physiological effects and mode of action of ZnO nanoparticles against postharvest fungal contaminants. Food Res. Int., 2017, 101, 274-279.
[68] He L., Liu Y., Mustapha A., Lin M., Antifungal activity of zinc oxide nanoparticles against *Botrytis cinerea* and *Penicillium expansum*. Microbiol. Res., 2011, 166, 207-215.
[69] Majumdar S., Roy A., Nandi I., Banerjee P., Banerjee S., Ghosh M., Chakrabarti S., Paper coated with sonochemically synthesized zinc oxide nanoparticles: Enhancement of properties for preservation of documents. Tappi J., 2017, 16, 25-33.
[70] Arciniegas-Grijalba P.A., Patiño-Portela M.C., Mosquera-Sánchez L.P., Guerrero-Vargas J.A., Rodríguez-Páez J. E., ZnO nanoparticles (ZnO-NPs) and their antifungal activity against coffee fungus *Erythricium salmonicolor*. Appl. Nanosci., 2017, 7, 225–241.
[71] Sardella D., Gatt R., Valdramidis V.P., Assessing the efficacy of zinc oxide nanoparticles against *Penicillium expansum* by automated turbidimetric analysis. Mycology., 2017, 1-6. https://doi.org/10.1080/21501203.2017.1369187.
[72] Jaffri S.B., Ahmad K.S., Augmented photocatalytic, antibacterial and antifungal activity of prunosynthetic silver nanoparticles. Artif. Cells Nanomed. Biotechnol., 2017, 1-11. https://doi.org/10.1080/21691401.2017.1414826
[73] Ahmad K.S., Rashid N., Tazaiyen S., Zakria M., Sorption-Desorption Characteristics of Benzimidazole Based Fungicide 2-(4-fluorophenyl)-1H-benzimidazole on Physicochemical Properties of Selected Pakistani Soils. J. Chem. Soc. Pakistan., 2014, 36, 1189-1195.
[74] Ahmad K.S., Rashid N., Sorption-Desorption Behavior of Newly synthesized N-(1H-Benzimidazole-2 ylmethyl) Acetamide (ABNZ) on Selected Soils and its Antifungal activity. J. Chem. Soc. Pakistan., 2015, 37, 841-849.